Archival Report

Biological Psychiatry

Sleep Deprivation Effects on Brain State Dynamics Are Associated With Dopamine D_2 Receptor Availability Via Network Control Theory

Rui Zhang, Sukru Baris Demiral, Dardo Tomasi, Weizheng Yan, Peter Manza, Gene-Jack Wang, and Nora D. Volkow

ABSTRACT

BACKGROUND: Sleep deprivation (SD) negatively affects brain function. Most brain imaging studies have investigated the effects of SD on static brain function. SD effects on functional brain dynamics and their relationship with molecular changes remain relatively unexplored.

METHODS: We used functional magnetic resonance imaging to examine resting-brain state dynamics after one night of SD compared with rested wakefulness (N = 41) and assessed the association of brain state dynamics with striatal brain dopamine D_2 receptor availability measured by positron emission tomography [^{11}C]raclopride using network control theory.

RESULTS: SD reduced dwell time and persistence probabilities, with the strongest effects in two brain states, one characterized by high default mode network and low dorsal attention network activity and the other by high frontoparietal network and low somatomotor network activity. Using network control theory, we showed that after SD, there was an overall increase in the control energy required for brain state transitions, with effects varying for different brain state transitions. Control energy requirement was negatively associated with transition probabilities under SD and restful wakefulness and accounted for SD-induced changes in transition probabilities. Alteration in the energy landscape was associated with SD-induced changes in striatal D_2 receptor distribution.

CONCLUSIONS: These findings demonstrate altered occurrence of internally and externally oriented brain states following acute SD and suggest an association with energy requirements for brain state transitions modulated by striatal D_2 receptors.

https://doi.org/10.1016/j.biopsych.2024.08.001

Acute sleep deprivation (SD) that lasts 24 to 48 hours negatively impacts brain function, affecting cognition, emotions, reward processing, and incentive-driven behaviors (1). These adverse effects are believed to arise from an SD-induced imbalance in brain networks and erratic arousal activity (1). One brain network particularly susceptible to the effects of SD is the default mode network (DMN), which is highly active during rest. SD disrupts DMN connectivity by reducing its within-network integration (2) and its segregation from the dorsal attention network (DAT) (3). Most functional magnetic resonance imaging (MRI) studies of SD have focused on static resting-state functional connectivity (RSFC), whereas there has been limited research on the effects of SD on brain temporal dynamics, which may underlie critical aspects of cognition and behavior (4). One study that evaluated dynamic RSFC reported reduced dwell time in states characterized by anticorrelation between the DMN and other brain regions after SD (5).

In addition to consistent findings from RSFC studies on the DMN's sensitivity to SD, various studies have documented the contribution of dopamine to the effects of SD (1,6). Specifically, using positron emission tomography (PET), studies have shown that one night of SD reduced striatal dopamine D_2 receptor (D2R) availability, which accounted for altered brain activation during a visual attention task (6,7). A follow-up study further showed that reduced D2R binding after SD reflected receptor downregulation rather than dopamine increases, suggesting that D2R internalization could play an important role in modulating wakefulness (8). Importantly, evidence points to striatal D2R's influencing spontaneous brain activity in the absence of a stimulus or task, with the DMN exhibiting the most robust associations (9,10).

We considered these convergent findings and posited that SD would exert a significant effect on resting-brain functional dynamics by modulating striatal D2R availability. Specifically, we anticipated that SD would alter brain state transitions. DMN-dominated states would be the brain states most susceptible to SD, such that there would be less time spent in the DMN state and increases in transitions from the DMN state to other brain states under SD. We also hypothesized that altered brain state dynamics following SD would be modulated by striatal D2R-induced changes in energy landscapes. The role of striatal D2R in arousal is well recognized. Studies on D2R

knockout mice have shown decreased arousal (11), and human studies have reported that SD-induced reductions in striatal D2R were associated with sleepiness (8). Therefore, we expected that SD-induced changes in striatal D2R would modulate brain state dynamics by decreasing arousal and increasing overall energy barriers for brain state transitions.

To test these hypotheses, we applied network control theory, a mathematic tool that models brain state dynamics as a function of brain structure and control energy (energy required to transition from one brain state to another) (12,13). In this study, we aimed to 1) assess SD-induced changes in brain state dynamics using a data-driven clustering approach to identify brain states (whole-brain network activation pattern) at a single time frame, 2) examine SD-induced changes in the energy landscape that calculates the minimum energy needed to transition between different brain states or maintain the same brain state based on normative structural connectome data obtained from diffusion MRI, 3) test whether SD-induced changes in control energy are associated with SD-induced changes in brain state transition probability (14), and 4) investigate whether SD-induced changes in energy landscape can be explained by striatal D2R changes following SD. ΔD2R maps were calculated as percentage changes following SD in contrast to rested wakefulness (RW) using [^{11}C]raclopride PET data. Because a smaller number of control nodes/inputs will always lead to higher control energy in network control theory, here we investigated the effect of SD-induced distribution changes in striatal D2R rather than absolute changes in striatal D2R availability on control energy.

METHODS AND MATERIALS

Participants

This study included 41 healthy participants (mean age ± SD = 41.16 ± 13.14 years, 22 female, 51% Black, 41% White) who spent 2 nights at the National Institutes of Health's clinical center. The order of SD and RW conditions were counterbalanced across participants and were 12.80 ± 10.02 days apart on average. If the SD condition was performed prior to the RW condition, the protocol specified that there had to be at least 7 days between the 2 sessions. The MRI scans were performed between 8 AM and 12 PM for both the SD and RW conditions (average scan start time = 8:30 AM). Written informed consent approved by the Institutional Review Board at the National Institutes of Health was obtained from all participants. See the Supplement for exclusion criteria and study procedures.

MRI Acquisition and Preprocessing

See the Supplement for details on MRI acquisition.

The data were preprocessed using CONN toolbox 21a (15) including rigid body realignment, spatial normalization to Montreal Neurological Institute space, smoothing (full width at half maximum = 6 mm), bandpass filtering (0.01–0.08 Hz), linear detrending, head motion regression (3 rotational, 3 translational and their derivatives), and removal of signals within the cerebrospinal fluid and the white matter (WM) using aCompcor, a method for identifying principal components associated with segmented WM and cerebrospinal fluid. Using custom MATLAB (version R2022b; The MathWorks, Inc.) code, we further removed volumes with a framewise displacement threshold of 0.25 mm and DVARS threshold of 150%. After scrubbing, framewise displacement for the SD condition was 0.12 ± 0.02, and for the RW condition, it was 0.10 ± 0.02.

Analysis of Brain States and Dynamics

To identify brain states, i.e., brain coactivation patterns, denoised voxel-level data (percent signal changes) were first parcellated into an augmented 232-node Schaefer atlas (200 cortical regions of interest [ROIs] and 32 subcortical ROIs that included regions from the hippocampus, amygdala, thalamus, and striatum) (16,17), and each ROI time series was demeaned. Then, we concatenated demeaned ROI time series from all participants and conditions (matrix row: $N_{participants} \times N_{time\ points}$; column: N_{ROIs}) and applied k-means clustering (14). The optimal number of clusters (k) $k = 6$ was chosen because the additional variance explained by increasing k beyond $k = 6$ was <1%. (Figure S1). Please see the Supplement for details.

Next, we analyzed the dynamic characteristics of the identified brain states. The fractional occupancy was defined as the proportion of repetition times assigned to each brain state. Dwell time was calculated by averaging the length of time spent in a brain state. Appearance rate was determined by the total number of times a state appeared per minute. Additionally, transition probability between states i and j was defined as the probability that state j occurs at the repetition time after state i, given that state i is occurring.

Complexity/Entropy Index

We calculated two complexity/entropy indices, one based on the brain state time series and the other on the blood oxygen level–dependent (BOLD) time series. For the former index, the more complex the brain state transition pattern, the less predictable and more entropic it is (18,19). For the latter index, a higher value indicates less self-similarity and greater brain activity entropy (20). See the Supplement for details about calculation.

Structural Connectivity Network Construction

Diffusion MRI data for 1201 participants from the Human Connectome Project were used to construct a population-level structural connectome, which has been made publicly available by Yeh *et al.* (21,22). We applied the same approach as described in (23) to construct a volume-normalized structural connectome with the Schaefer 232 atlas. See the Supplement for network construction.

ΔD2R Mapping

[^{11}C]raclopride PET data from 20 healthy male control participants were used to map D2R changes induced by SD. Details for study procedures, PET scan, and analyses have been reported previously (24). For each condition (RW, SD), we estimated the distribution volume ratio (DVR) for each voxel and used the cerebellum as a reference region. Based on an individual's DVR images, we then calculated ΔD2R DVR maps for SD-induced percentage changes of D2R availability, i.e., (SD − RW)/RW for each participant. Finally, ΔD2R DVR maps were averaged and parcellated into Schaefer atlases (16,17).

Energy Calculations

Network control theory advances our understanding of how WM structure constrains brain dynamics and allows us to compute the minimum energy required for brain state transitions and persistence given the WM connections (14). Here, we applied network control theory to 1) understand how SD alters the minimum energy requirement for brain state transitions assuming that there were no WM changes after one night of SD and 2) assess whether changes in the minimum energy requirement can be explained by SD-induced striatal ΔD2R. We employed a linear time-invariant model:

$$\dot{x}(t) = Ax(t) + Bu(t) \quad (1)$$

where x is the brain regional activity at time t, A describes NxN structural connectome, N is the number of brain regions, and B contains the control input weights for each brain region, i.e., how much energy can be injected into a specific brain region. In the current study, we calculated minimum control energy under 3 conditions in which the B matrix varied. Model 1 (for RW and SD conditions): uniformly weighted inputs from all 232 regions (diagonal values in B identity matrix were 1). Model 2 (for RW and SD conditions): uniformly weighted inputs from 12 striatal regions (diagonal values in B matrix were 1 for 12 striatal regions and 0 for other regions). Model 3 (for RW condition only): SD-induced ΔD2R weighted control inputs from 12 striatal regions. Striatal ΔD2Rs were scaled such that the minimum value was 1 and then normalized such that the mean of 12 striatal ROIs was 1 and the sum was 12. The purpose of normalization was to make sure that models 2 and 3 had the same amount of control inputs. We compared models 2 and 3 for the RW condition to investigate how SD-induced striatal ΔD2R affects control energy. u is the control energy being injected over time. See the Supplement for calculating the minimum control energy and calculating control energy for each brain region.

Analysis of Static Functional Connectivity

Denoised voxel-level data were used for analyses. Pearson's correlation coefficients between the ROIs' time courses were computed. Correlation coefficients were then converted to normally distributed *z* scores using the Fisher transformation. We then calculated between-network and within-network RSFC for the SD and RW conditions.

Statistical Analysis

The ΔD2R-weighted inputs from the true receptor distribution were compared with the randomly shuffled (12 striatal regions) via a permutation test and the energy matrix recalculated 10,000 times. *p* Values were calculated as the fraction of times that the randomized distribution resulted in a higher energy than the true distribution. All other metric comparisons between the SD and RW conditions were achieved using 2-sided paired *t* tests and were corrected for multiple comparisons with Benjamini-Hochberg when correction was indicated. Spearman correlations were used for correlations between control energy and transition probability.

RESULTS

Brain States

To understand the spatiotemporal dynamics of brain activity, we applied a data-driven clustering approach to identify the whole-brain coactivation patterns at single time frames and then quantified their dynamics (14). Recurrent coactivation patterns were referred to as brain states, and we identified 6 brain states (Figure 1) that were highly similar under the RW and SD conditions (Figure S2). Based on the predominance of the network patterns in each brain state, the 6 brain states were labeled as somatomotor (SOM+, SOM−), visual (VIS+, VIS−), default mode (DMN+), and visual attention (VAT+), with (+) and (−) indicating activity above or below regional means, respectively.

SD Affects Brain State Dynamics and Transition Probabilities

To capture dynamic characteristics of the identified brain states, we calculated fractional occupancy (probability of occurrence), dwell time (duration of persistence), and appearance rates (frequency of appearance per minute) of each state under the SD and RW conditions. Additionally, we computed transition probability between brain states, complexity of brain state transition patterns, and brain activity entropy.

SD decreased fractional occupancy in DMN+ and dwell time in DMN+, SOM+, SOM−, and VIS−, whereas it increased fractional occupancy in VIS+ (Figure 2A). Regarding transition probabilities, SD reduced the probability of persistence in a brain state except for VIS+. In contrast, transition probabilities between different brain states were increased after SD, particularly between VIS and SOM states and from DMN+ to VIS+/VAT+ states (Figure 2B). Figure S3 shows brain state transition probabilities when excluding self-transitions. SD increased the complexity of brain state transition pattern (t_{40} = 4.36, $p < .001$) (Figure 2C). Likewise, brain activity entropy calculated based on BOLD time series increased after SD (t_{40}= 3.91, $p < .001$) (Figure S4).

Head motion under SD was greater than under RW (t_{40} = 5.6, $p < .001$). Although we restrictedly corrected for head motion, we also examined how changes in head motion might have contributed to the observed changes in brain state dynamics. Head motion, i.e., framewise displacement, was associated with lower dwell time in SOM states and greater fractional occupancy in the VIS+ state. DMN+ and VAT+ states and brain transition complexity were less affected by head motion (Figure S5).

SD Altered Control Energies That Were Associated With Transition Probabilities

We applied network control theory to calculate the control energy, which is the minimum energy needed for transition between brain states. The control energy required to maintain each state is referred to as persistence energy, and the control energy required to change states is referred to as transition energy. Using this framework, previous studies have shown that the brain favors transitions to brain states that require less control energy (14,23). According to the network control theory, energy is injected into the system at control points to induce the desired transition. First, we allowed the control inputs to be uniformly weighted from all brain regions (model 1). Compared with RW, SD increased the control energy needed to transition between brain states and the persistence energy needed to maintain each state (Figures 3A and S6A). Similar energy increases were observed except for transition energies

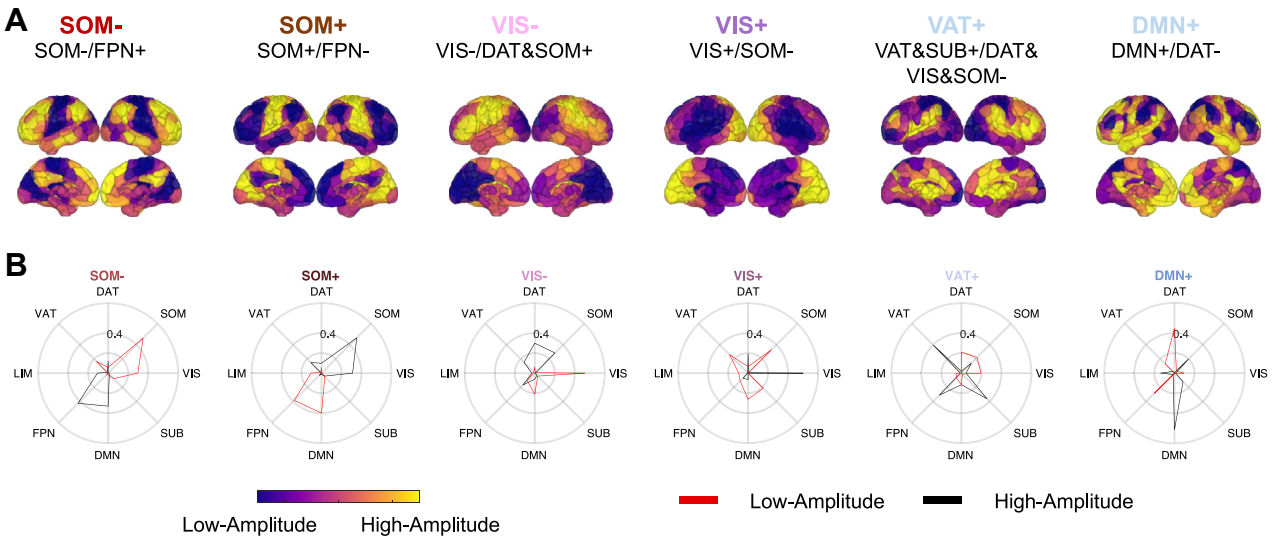

Figure 1. Recurrent brain states. **(A)** Brain states were identified using a data-driven approach and labeled based on the cosine similarity with a priori–defined resting-state functional networks. Anatomical representation of brain states with their centroids mapped to colors of the corresponding 232 regions of the Schaefer atlas consisting of 200 cortical and 32 subcortical regions. Centroids of each state were calculated as the mean of the regional activation over all repetition times assigned to that state. The top label reflects resting-state functional networks with the most overall similarity, and the bottom label reflects the resting-state functional networks with the most similarity to the high- and low-amplitude activity of each state, respectively. + and − represent activity above or below regional means, respectively. **(B)** Radial plot of each brain state represents cosine similarity of its high-amplitude and low-amplitude activity with resting-state functional networks. Larger values correspond to higher similarity. DAT, dorsal attention network; DMN, default mode network; FPN, frontoparietal network; LIM, limbic network; SOM, somatomotor network; SUB, subcortical region; VAT, ventral attention network; VIS, visual network.

between SOM+ and VIS+, between DMN+ and VAT+, and for persistence energy for VIS+ when only allowing uniformly weighted control inputs from 12 striatal regions (model 2) (Figure 3C). Consistent with previous findings (14,23), we found that control energy was negatively associated with empirically observed brain state transition probability under

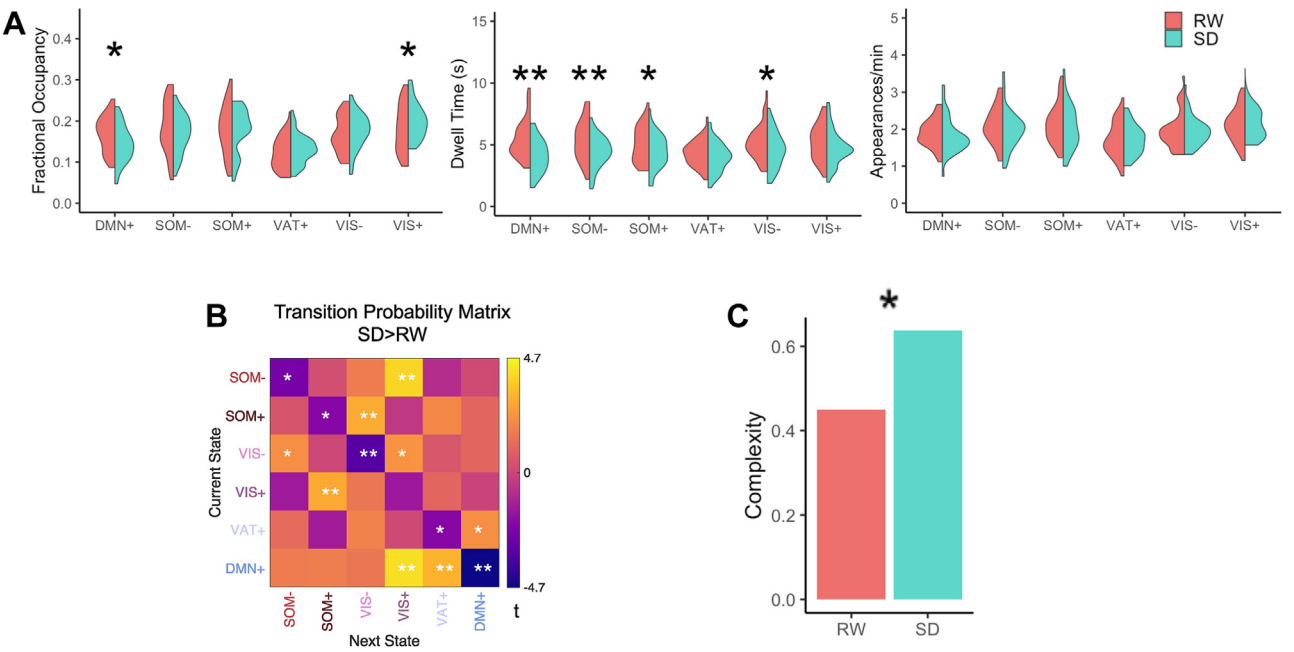

Figure 2. Brain state dynamics modulated by sleep deprivation (SD). **(A)** Fractional occupancy, dwell time, and appearance rate of each brain state under SD and rested wakefulness (RW). **(B)** Brain state transition probabilities including persistence probabilities following SD compared with RW. *t* Values are represented. **(C)** Complexity of brain state transitions. Condition comparisons (SD vs. RW) were performed using 2-sided paired *t* tests. *uncorrected $p < .05$, **Benjamini-Hochberg–corrected $p < .05$. DMN, default mode network; SOM, somatomotor network; VAT, ventral attention network; VIS, visual network.

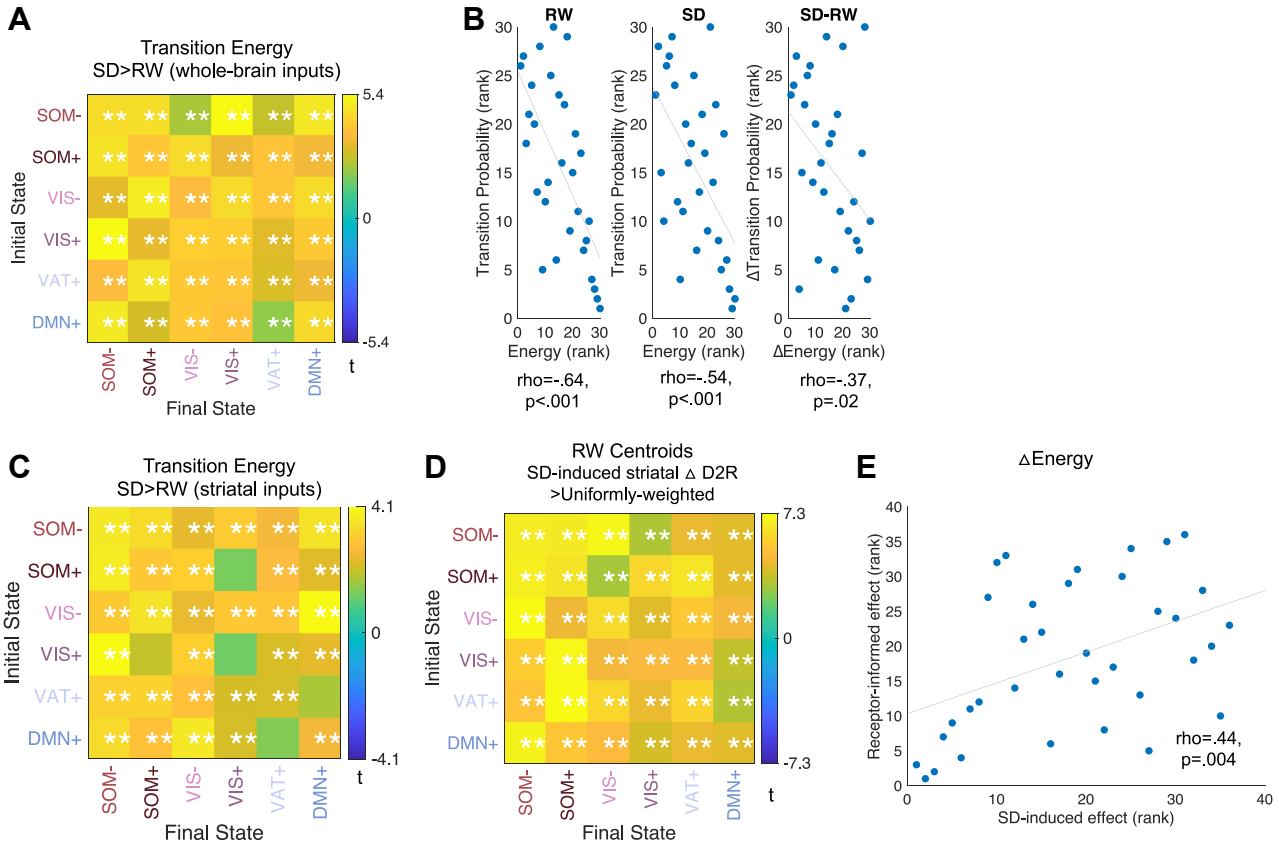

Figure 3. Increases in control energy after sleep deprivation (SD) are negatively associated with brain state transition probability and are contributed to by changes in striatal dopamine D_2 receptors (D2Rs). **(A)** Condition comparisons (SD > rested wakefulness [RW]) of structure-based brain state transition energy prediction calculated with uniformly weighted whole-brain inputs. SD brain states required higher energy to maintain or transition between each state than RW brain states. **(B)** Energy requirement is negatively associated with transition probability under the RW (left) and SD condition (middle). Required energy changes also accounts for condition differences in brain state transition probability (right). Energy (E) change is calculated as $(E_{SD} - E_{RW})/E_{RW}$. Persistence energy for each state is very low and not included in the figure. **(C)** Condition comparisons (SD > RW) of structure-based brain state transition energy prediction calculated with uniformly weighted striatal inputs. **(D)** Compared with uniformly weighted striatal inputs, weighting the striatal inputs by SD-induced D2R changes leads to significant increases in the energy required for the transitions/persistence among RW brain states (centroids). **(E)** Positive correlation between SD-induced and receptor-informed changes in control energy, i.e., comparison of **(C)** and **(D)**. Color bar represents the *t* value from paired *t* tests. *uncorrected $p < .05$, **Benjamini-Hochberg–corrected $p < .05$. DMN, default mode network; SOM, somatomotor network; VAT, ventral attention network; VIS, visual network.

RW and SD conditions (Figure 3B). The extent of energy increases was negatively associated with SD-induced changes in brain state transition probabilities (Figure 3B). See the Supplement for regional control energy results.

To investigate where differences in control energy were due to differences in the spatial patterns and not driven by differences in amplitude (centroids) of the brain states, we normalized the brain states using L2 normalization and recalculated control energies. The findings suggested that transition energies between VIS− and SOM+/− and between VAT+ and DMN+ were strongly influenced by differences in the spatial patterns (Figures S6B and S7B).

Contribution of SD-Induced Striatal D2R Changes to Control Energy

We hypothesized that the higher control energy requirement under the SD condition than under the RW condition could be the result of altered striatal D2R distribution following SD. Our previous work had documented how striatal D2R binding changed between the RW and the SD conditions (6,7). Using this information, we tested whether changing striatal D2R distribution under RW would lead to a similar energy landscape as was observed under the SD condition.

We found that ΔD2R-weighted striatal inputs for the RW condition (model 3) (Figure S11) resulted in higher control energy than uniformly weighted inputs for the RW condition (model 2) (Figure 3D). There was a positive correlation between SD-induced and receptor-informed effects on control energy (Figure 3E). Additionally, we compared the control energy obtained from the true SD-induced striatal ΔD2R distribution versus that from a permutated striatal ΔD2R map. The true distribution of the striatal ΔD2R map led to significantly higher energy needed for brain state transitions than that from the permutation map (Figure S12).

The Effect of SD on Global Signal Amplitude

Because reduced vigilance was associated with higher amplitude of BOLD activity in previous studies (25), we compared the global signal amplitude between the RW and SD conditions. A global mean signal was defined as the average of the BOLD signals across 232 ROIs. The standard deviation of the global signal was defined as the global signal amplitude (26). The global signal amplitude did not differ between the SD and RW conditions (t_{40} = 0.67, p = .507).

The Effect of SD on RSFC

SD decreased between-network RSFC, particularly between subcortical and cortical networks and between VAT/DAT and SOM/VIS and decreased anticorrelation between DMN and VAT (Figure S13). Decreased within-network RSFC was observed in VIS, SOM, DAT, and VAT (Figure S13).

DISCUSSION

The current study advances our mechanistic understanding of the effects of SD on brain function by revealing 1) changes in brain state dynamics at rest, 2) increases in the control energy required for brain state transitions and for state persistence under the framework of network control theory, and 3) linkage between SD-induced changes in brain state dynamics and distribution of striatal ΔD2R mediated by altered energy landscapes.

SD Effects on Brain State Dynamics

SD reduced dwell time and persistence probabilities of recurrent brain states, with the strongest effect in DMN+ and SOM−. With our approach, the DMN+ state was characterized by contra-activation of DMN (high activity) and DAT (low activity), and SOM− was characterized by contra-activation of SOM (low activity) and the frontoparietal network (high activity). Using a sliding-window approach, a previous study showed reduced dwell time in states characterized by anticorrelation between the DMN and other brain regions after SD (5). A similar finding was reported in another study that demonstrated that a dynamic functional connectivity state with reduced within-network RSFC of the DMN, VAT, and DAT and weaker anticorrelation between these networks was associated with low arousal after SD (27). Therefore, our findings are consistent with previous studies highlighting the disrupted dynamics of the DMN, an internally oriented network, and the DAT, an externally oriented network, and impaired cognitive control for processing sensorimotor inputs after SD (28). Our static RSFC analyses revealed decreased within-network RSFC in the VIS, SOM, DAT, and VAT. Consistent with previous studies, we also found decreased anticorrelation between DMN and VAT following SD. Additionally, we observed reduced between-network RSFCs, particularly between subcortical networks and cortical networks, which could affect motor, cognitive, and emotional regulation (29–31), while decreased RSFC between VAT/DAT and SOM/VIS may contribute to impaired attentional processes associated with sleep loss (32). Furthermore, our results documented greater brain entropy after SD, i.e., the transition patterns became more complex and unpredictable than RW. Apart from brain state transitions, increased brain entropy was also observed for regional BOLD time series following SD. The extent to which SD induced changes in brain state dynamics underlies the neural underpinnings of disrupted mind wandering or impairments in sustaining attention that have been reported following SD merits further investigation (33,34). In this study, SD did not affect global signal amplitude, which was associated with vigilance in previous studies (26), indicating that reduced alertness is less likely to account for observed changes in brain state dynamics.

The Effect of SD on Control Energy and Its Association With Brain State Dynamics

SD increased the overall control energy needed for brain state transition and for brain state persistence. The extent of energy increases differed in brain state transitions. Changes in control energy after SD were primarily explained by changes in the amplitude of brain states, with some exceptions, including transition energies between the VIS− and SOM+/− and between the VAT+ and DMN+ that were significantly influenced by differences in the spatial patterns of brain states. Studies have suggested a negative correlation between control energy calculated with network control theory and PET-derived measures of brain glucose metabolism as observed in temporal lobe epilepsy (35) and schizophrenia (14,36). This computational evidence obtained from network control theory was consistent with brain metabolic findings with SD showing reduced cerebral glucose metabolism. Specifically, PET studies with fluorodeoxyglucose showed that 24 hours of SD led to a significant decrease in global cerebral glucose metabolism with regional differences in the magnitude of these reductions (37–39). SD-induced changes in global and relative regional glucose metabolic activity may contribute to increases in global and regional control energy and to the different energy requirements for distinct brain state transitions after SD. Moreover, the degree of heightened control energy subsequent to SD exhibited a negative correlation with SD-triggered alterations in transition probabilities among brain states, consistent with previous investigations that employed network control theory (14,23,40). Similarly, regions with the most substantial increases in control energy showed the least augmentation in brain activity entropy following SD (Figure S9). In contrast, individuals with the greatest increases in global control energy showed the most pronounced escalation in brain activity entropy (Figure S10A). This finding contradicted earlier findings that demonstrated inverse relationships between transition energy changes and either brain activity or brain state transition entropy (23,41). In the current study, individuals demonstrating the most significant SD-induced changes in global control energy showed the greatest regional diversity in control energy (Figure S10C) and entropy increases (Figure S10D). Such variations could potentially influence overall associations between global control energy and averaged brain entropy. The finding may indicate individual differences in compensatory brain mechanisms following SD, wherein certain regions adapt to become more intricate and adaptable, while others tend toward stability in brain responses to uphold certain performance levels.

Associations Between SD-Induced Changes in D2Rs and Control Energy

In the current study, changes in striatal D2Rs following SD resulted in control energy increases. ΔD2R-stimulated

increases in control energy were positively associated with SD-induced empirical control energy increases. Positive associations between striatal D2R and brain glucose metabolism have been documented in Parkinson's disease (42), obesity (43), cocaine addiction (44), and healthy aging (45). The observed associations of ΔD2R with increased control energy could be related to its associations with reduced brain glucose metabolism after SD.

Limitations

The current study calculated control energy under the framework of network control theory through conceptual modeling, which differs from glucose metabolic cost that has neurobiological underpinnings and is measured by PET fluorodeoxyglucose. However, as discussed above, these two measures may be closely correlated and need future investigations. Also, SD influences other receptors in addition to D2Rs, such as increasing cerebral 5-HT_{2A} receptors (46) and adenosine A_1 receptors (47) that modulate brain activity and connectivity (48). A model that includes multireceptor information may yield better prediction of SD-induced changes in control energy and brain dynamics. In our model, we assumed that WM structure has minimum impact on control energy changes following SD. However, WM microstructure in healthy participants may be affected by one night of SD (49). Finally, to map the regional brain changes in D2Rs from SD, we used an average ΔD2R map obtained from a previous study (24), so we were unable to determine the extent to which at an individual level, the changes in D2R availability with SD predict changes in brain state dynamics during SD for that person. The affinity of [^{11}C]raclopride for D2R is relatively low, thus, the specific to nonspecific signal in extrastriatal regions provided by [^{11}C]raclopride is lower than other radiotracers such as [^{11}C]fallypride (50,51). For this reason, we only used striatal D2Rs in our analyses. It would be relevant to investigate the contribution of cortical D2R in future studies.

Conclusions

The current study uncovered high-temporal brain state dynamics changes following one night of SD, highlighting disrupted dynamics between internally and externally oriented brain states. The dynamic changes were associated with an altered energy landscape contributed to by SD-induced changes in striatal D2R distribution.

ACKNOWLEDGMENTS AND DISCLOSURES

This work was supported by the National Institute on Alcohol Abuse and Alcoholism (Grant No. ZIAAA000550 [principal investigator, NDV]).

All authors report no biomedical financial interests or potential conflicts of interest.

ARTICLE INFORMATION

From the Laboratory of Neuroimaging, National Institute on Alcohol Abuse and Alcoholism, National Institutes of Health, Bethesda, Maryland.

Address correspondence to Rui Zhang, Ph.D., at rui.zhang@nih.gov, or Nora D. Volkow, M.D., at nvolkow@nida.nih.gov.

Received Sep 19, 2023; revised Jul 28, 2024; accepted Aug 2, 2024.

Supplementary material cited in this article is available online at https://doi.org/10.1016/j.biopsych.2024.08.001.

REFERENCES

1. Krause AJ, Ben Simon EB, Mander BA, Greer SM, Saletin JM, Goldstein-Piekarski AN, Walker MP (2017): The sleep-deprived human brain. Nat Rev Neurosci 18:404–418.
2. Gujar N, Yoo S-S, Hu P, Walker MP (2010): The unrested resting brain: Sleep deprivation alters activity within the default-mode network. J Cogn Neurosci 22:1637–1648.
3. De Havas JA, Parimal S, Soon CS, Chee MWL (2012): Sleep deprivation reduces default mode network connectivity and anti-correlation during rest and task performance. Neuroimage 59:1745–1751.
4. Hutchison RM, Womelsdorf T, Allen EA, Bandettini PA, Calhoun VD, Corbetta M, *et al.* (2013): Dynamic functional connectivity: Promise, issues, and interpretations. Neuroimage 80:360–378.
5. Xu H, Shen H, Wang L, Zhong Q, Lei Y, Yang L, *et al.* (2018): Impact of 36 h of total sleep deprivation on resting-state dynamic functional connectivity. Brain Res 1688:22–32.
6. Tomasi D, Wang GJ, Volkow ND (2016): Association between striatal dopamine D2/D3 receptors and brain activation during visual attention: Effects of sleep deprivation. Transl Psychiatry 6:e828.
7. Volkow ND, Wang G-J, Telang F, Fowler JS, Logan J, Wong C, *et al.* (2008): Sleep deprivation decreases binding of [11C]raclopride to dopamine D2/D3 receptors in the human brain. J Neurosci 28:8454–8461.
8. Volkow ND, Tomasi D, Wang G-J, Telang F, Fowler JS, Logan J, *et al.* (2012): Evidence that sleep deprivation downregulates dopamine D2R in ventral striatum in the human brain. J Neurosci 32:6711–6717.
9. Zhang R, Volkow ND (2019): Brain default-mode network dysfunction in addiction. Neuroimage 200:313–331.
10. Ionescu TM, Amend M, Hafiz R, Biswal BB, Maurer A, Pichler BJ, *et al.* (2021): Striatal and prefrontal D2R and SERT distributions contrastingly correlate with default-mode connectivity. Neuroimage 243:118501.
11. Qu W-M, Xu X-H, Yan M-M, Wang Y-Q, Urade Y, Huang Z-L (2010): Essential role of dopamine D2 receptor in the maintenance of wakefulness, but not in homeostatic regulation of sleep, in mice. J Neurosci 30:4382–4389.
12. Gu S, Pasqualetti F, Cieslak M, Telesford QK, Yu AB, Kahn AE, *et al.* (2015): Controllability of structural brain networks. Nat Commun 6:8414.
13. Kim JZ, Soffer JM, Kahn AE, Vettel JM, Pasqualetti F, Bassett DS (2018): Role of graph architecture in controlling dynamical networks with applications to neural systems. Nat Phys 14:91–98.
14. Cornblath EJ, Ashourvan A, Kim JZ, Betzel RF, Ciric R, Adebimpe A, *et al.* (2020): Temporal sequences of brain activity at rest are constrained by white matter structure and modulated by cognitive demands. Commun Biol 3:261.
15. Whitfield-Gabrieli S, Nieto-Castanon A (2012): Conn: A functional connectivity toolbox for correlated and anticorrelated brain networks. Brain Connect 2:125–141.
16. Schaefer A, Kong R, Gordon EM, Laumann TO, Zuo X-N, Holmes AJ, *et al.* (2018): Local-global parcellation of the human cerebral cortex from intrinsic functional connectivity MRI. Cereb Cortex 28:3095–3114.
17. Tian Y, Margulies DS, Breakspear M, Zalesky A (2020): Topographic organization of the human subcortex unveiled with functional connectivity gradients. Nat Neurosci 23:1421–1432.
18. Ritschard G (2023): Measuring the nature of individual sequences. Sociol Methods Res 52:2016–2049.
19. Gabadinho A, Ritschard G, Müller NS, Studer M (2011): Analyzing and visualizing state sequences in R with TraMineR. J Stat Softw 40:1–37.
20. Richman JS, Moorman JR (2000): Physiological time-series analysis using approximate entropy and sample entropy. Am J Physiol Heart Circ Physiol 278:H2039–H2049.
21. Van Essen DC, Smith SM, Barch DM, Behrens TEJ, Yacoub E, Ugurbil K, WU-Minn HCP Consortium (2013): The WU-Minn Human connectome Project: An overview. Neuroimage 80:62–79.
22. Yeh F-C, Panesar S, Fernandes D, Meola A, Yoshino M, Fernandez-Miranda JC, *et al.* (2018): Population-averaged atlas of the macroscale human structural connectome and its network topology. Neuroimage 178:57–68.

23. Singleton SP, Luppi AI, Carhart-Harris RL, Cruzat J, Roseman L, Nutt DJ, *et al.* (2022): Receptor-informed network control theory links LSD and psilocybin to a flattening of the brain's control energy landscape. Nat Commun 13:5812.
24. Volkow ND, Wang GJ, Logan J, Alexoff D, Fowler JS, Thanos PK, *et al.* (2015): Caffeine increases striatal dopamine D2/D3 receptor availability in the human brain. Transl Psychiatry 5:e549.
25. Liu TT, Falahpour M (2020): Vigilance effects in resting-state fMRI. Front Neurosci 14:321.
26. Wong CW, Olafsson V, Tal O, Liu TT (2013): The amplitude of the resting-state fMRI global signal is related to EEG vigilance measures. Neuroimage 83:983–990.
27. Wang C, Ong JL, Patanaik A, Zhou J, Chee MWL (2016): Spontaneous eyelid closures link vigilance fluctuation with fMRI dynamic connectivity states. Proc Natl Acad Sci USA 113:9653–9658.
28. Ning Y, Zheng S, Feng S, Yao H, Feng Z, Liu X, *et al.* (2022): The altered intrinsic functional connectivity after acupuncture at shenmen (HT7) in acute sleep deprivation. Front Neurol 13:947379.
29. Li B-Z, Cao Y, Zhang Y, Chen Y, Gao Y-H, Peng J-X, *et al.* (2021): Relation of decreased functional connectivity between left thalamus and left inferior frontal gyrus to emotion changes following acute sleep deprivation. Front Neurol 12:642411.
30. Feng P, Becker B, Zheng Y, Feng T (2018): Sleep deprivation affects fear memory consolidation: Bi-stable amygdala connectivity with insula and ventromedial prefrontal cortex. Soc Cogn Affect Neurosci 13:145–155.
31. Wang H, Yu K, Yang T, Zeng L, Li J, Dai C, *et al.* (2021): Altered functional connectivity in the resting state neostriatum after complete sleep deprivation: Impairment of motor control and regulatory network. Front Neurosci 15:665687.
32. Killgore WDS (2010): Effects of sleep deprivation on cognition. Prog Brain Res 185:105–129.
33. Cárdenas-Egúsquiza AL, Berntsen D (2022): Sleep well, mind wander less: A systematic review of the relationship between sleep outcomes and spontaneous cognition. Conscious Cogn 102:103333.
34. Hudson AN, Van Dongen HPA, Honn KA (2020): Sleep deprivation, vigilant attention, and brain function: A review. Neuropsychopharmacology 45:21–30.
35. He X, Caciagli L, Parkes L, Stiso J, Karrer TM, Kim JZ, *et al.* (2022): Uncovering the biological basis of control energy: Structural and metabolic correlates of energy inefficiency in temporal lobe epilepsy. Sci Adv 8:eabn2293.
36. Townsend L, Pillinger T, Selvaggi P, Veronese M, Turkheimer F, Howes O (2023): Brain glucose metabolism in schizophrenia: A systematic review and meta-analysis of 18 FDG-PET studies in schizophrenia. Psychol Med 53:4880–4897.
37. Thomas M, Sing H, Belenky G, Holcomb H, Mayberg H, Dannals R, *et al.* (2000): Neural basis of alertness and cognitive performance impairments during sleepiness. I. Effects of 24 h of sleep deprivation on waking human regional brain activity. J Sleep Res 9:335–352.
38. Wu JC, Gillin JC, Buchsbaum MS, Hershey T, Hazlett E, Sicotte N, Bunney WE (1991): The effect of sleep deprivation on cerebral glucose metabolic rate in normal humans assessed with positron emission tomography. Sleep 14:155–162.
39. Wu JC, Gillin JC, Buchsbaum MS, Schachat C, Darnall LA, Keator DB, *et al.* (2008): Sleep deprivation PET correlations of Hamilton symptom improvement ratings with changes in relative glucose metabolism in patients with depression. J Affect Disord 107:181–186.
40. Braun U, Harneit A, Pergola G, Menara T, Schäfer A, Betzel RF, *et al.* (2021): Brain network dynamics during working memory are modulated by dopamine and diminished in schizophrenia. Nat Commun 12:3478.
41. Tozlu C, Card S, Jamison K, Gauthier SA, Kuceyeski A (2023): Larger lesion volume in people with multiple sclerosis is associated with increased transition energies between brain states and decreased entropy of brain activity. Netw Neurosci 7:539–556.
42. Nakagawa M, Kuwabara Y, Taniwaki T, Sasaki M, Koga H, Kaneko K, *et al.* (2005): PET evaluation of the relationship between D2 receptor binding and glucose metabolism in patients with parkinsonism. Ann Nucl Med 19:267–275.
43. Volkow ND, Wang G-J, Telang F, Fowler JS, Thanos PK, Logan J, *et al.* (2008): Low dopamine striatal D2 receptors are associated with prefrontal metabolism in obese subjects: Possible contributing factors. Neuroimage 42:1537–1543.
44. Volkow ND, Fowler JS, Wang GJ, Hitzemann R, Logan J, Schlyer DJ, *et al.* (1993): Decreased dopamine D2 receptor availability is associated with reduced frontal metabolism in cocaine abusers. Synapse 14:169–177.
45. Volkow ND, Logan J, Fowler JS, Wang GJ, Gur RC, Wong C, *et al.* (2000): Association between age-related decline in brain dopamine activity and impairment in frontal and cingulate metabolism. Am J Psychiatry 157:75–80.
46. Elmenhorst D, Kroll T, Matusch A, Bauer A (2012): Sleep deprivation increases cerebral serotonin 2A receptor binding in humans. Sleep 35:1615–1623.
47. Elmenhorst D, Meyer PT, Winz OH, Matusch A, Ermert J, Coenen HH, *et al.* (2007): Sleep deprivation increases A1 adenosine receptor binding in the human brain: A positron emission tomography study. J Neurosci 27:2410–2415.
48. Li C, Kroll T, Matusch A, Aeschbach D, Bauer A, Elmenhorst E-M, Elmenhorst D (2023): Associations between resting state brain activity and A1 adenosine receptor availability in the healthy brain: Effects of acute sleep deprivation. Front Neurosci 17:1077597.
49. Voldsbekk I, Groote I, Zak N, Roelfs D, Geier O, Due-Tønnessen P, *et al.* (2021): Sleep and sleep deprivation differentially alter white matter microstructure: A mixed model design utilising advanced diffusion modelling. Neuroimage 226:117540.
50. Svensson JE, Schain M, Plavén-Sigray P, Cervenka S, Tiger M, Nord M, *et al.* (2019): Validity and reliability of extrastriatal [11C]raclopride binding quantification in the living human brain. Neuroimage 202:116143.
51. Freiburghaus T, Svensson JE, Matheson GJ, Plavén-Sigray P, Lundberg J, Farde L, Cervenka S (2021): Low convergent validity of [11C]raclopride binding in extrastriatal brain regions: A PET study of within-subject correlations with [11C]FLB 457. Neuroimage 226:117523.